

The Dynamics of Thermal Annealing in Arsenic-Ion-Implanted GaAs

This content has been downloaded from IOPscience. Please scroll down to see the full text.

1996 Jpn. J. Appl. Phys. 35 L192

(<http://iopscience.iop.org/1347-4065/35/2B/L192>)

View [the table of contents for this issue](#), or go to the [journal homepage](#) for more

Download details:

IP Address: 140.113.38.11

This content was downloaded on 28/04/2014 at 14:49

Please note that [terms and conditions apply](#).

The Dynamics of Thermal Annealing in Arsenic-Ion-Implanted GaAs

Wen-Chung CHEN, Gong-Ru LIN and C.-S. CHANG

Institute of Electro-Optical Engineering, National Chiao Tung University, Hsinchu, Taiwan 300, Republic of China

(Received November 27, 1995; accepted for publication January 22, 1996)

The effect of thermal annealing on the surfaces of arsenic-ion-implanted GaAs has been investigated by transmission electron microscopy, deep level transient spectroscopy and temperature-dependent resistance measurements. For the annealed films of arsenic-ion-implanted GaAs arsenic precipitates and a band of deep-level defects with the activation energy of around 0.6 eV near the surface are observed. The mean size and concentration of As precipitates in samples implanted at a dosage of 10^{16} cm $^{-2}$ are about 2–3 nm and 7×10^{16} cm $^{-3}$, respectively. The cross section of the deep level defects near the surface is calculated to be 7×10^{-14} cm 2 . The carrier-transport mechanisms of both as-implanted GaAs and post-annealed GaAs are shown dominantly to be hopping type conduction and active type conduction, respectively.

KEYWORDS: arsenic-ion-implanted, GaAs, deep level transient spectroscopy, temperature-dependent resistance, transmission electron microscopy

In the past few years, arsenic-rich GaAs layers deposited by molecular beam epitaxy at low-temperature (LT-MBE) have attracted much attention because of their many desirable features, such as high resistivity for buffer layers and shorter carrier lifetime for photoconductor.¹⁾ The material is electrically conductive at room temperature but exhibits highly resistive characteristic after thermal annealing.²⁾ The LT-MBE GaAs film is also known to contain a large amount of arsenic antisite defects (As_{Ga}) which result from the excess of arsenic-related complexes incorporated in the epitaxial layer during the growth.³⁾ The carrier-transport mechanism of as-grown LT-MBE GaAs at temperatures below 300 K is dominated by hopping conduction. The origin is the presence of a large amount of an EL2-like deep-level defects in this material.⁴⁾ The high resistivity of the annealed LT-MBE GaAs is accompanied with precipitation of arsenic atoms during annealing. Either the model of defect compensation,⁴⁾ or the model of arsenic Schottky barrier,⁵⁾ has been proposed to explain the high resistivity.

In comparison to the LT-MBE GaAs layers, relatively less attention has been paid to the arsenic-ion-implanted (As^+ -implanted) GaAs which also contains an arsenic-rich layer.^{6–11)} The annealed As^+ -implanted GaAs layers have been found to be highly resistive and suitable for electrical isolation. And arsenic precipitates has also been observed in the post-annealed implanted sample by using transmission electron microscopy (TEM).⁸⁾ Recently, we have investigated carrier transport at the metal/semiconductor junction of the As^+ -implanted GaAs substrate. The major mechanism is the hopping conduction at temperature below 360 K.¹¹⁾ In this work, we studied the thermal annealing effect on the electrical characteristics of As^+ -implanted GaAs by using measurements of TEM, deep level transient spectroscopy (DLTS) and temperature-dependent resistance.

In our experiment, arsenic ions were implanted into the substrates (100) of the liquid encapsulated Czochralski grown semi-insulating (S.I.) GaAs with the implanting energy and dosage of 200 keV and 10^{16} atom·cm $^{-2}$, respectively. Some of the As^+ -implanted GaAs were

annealed at the temperature (T_a) 600°C for 30 minutes. Since the hopping conduction prevails in the as-implanted films, the films is conductive which may cause the large leakage current between the junction of metals and semiconductors.¹¹⁾ Thus a Schottky diode fabricated on the as-implanted film is not suitable for the measurements of DLTS. In order to measure the defects near the surface of the implanted samples, the metal-insulator-semiconductor (MIS) diodes were made on the implanted GaAs samples with Si_3N_4 of 130 nm thickness as insulator and with gold as Schottky contact. For temperature-dependent resistance measurements, two Ohmic contacts with gap of 35 micron were deposited on the implanted GaAs samples. In the measurements of DLTS the offset of reverse bias and the pulse of forward bias are -0.5 V and $+0.5$ V, respectively.

In the Fig. 1, the signal of DLTS at temperature around 380 K can only be observed for samples at $T_a = 600^\circ\text{C}$. The intensity of this signal from DLTS is proportional to the concentration of deep centers.¹⁷⁾ The activation energy (E_a) and cross section (σ) for sample annealed at 600°C are 0.6 eV and 7×10^{-14} cm 2 as calculated by the Arrhenius plot, which is shown in the inset of Fig. 1.^{13,14)} In Comparison with DLTS results from the earlier work of Look *et al.* on LT-MBE GaAs films, traps at the levels of 0.54 eV, 0.55 eV and 0.56 eV were found.¹²⁾ Besides, Xie *et al.* have demonstrated that in LT-MBE GaAs an electron trap at 0.58 eV below the conduction band as a dominant level which is related to the formation of arsenic precipitates.¹⁷⁾ In boron-implanted GaAs, a complex defect with its $E_a = 0.55$ eV was also observed by implanting process.¹⁸⁾ The EL3 in vapor-phase-epitaxial GaAs with $E_a = 0.575$ eV has been found to exist in arsenic-rich growth processes, it may be related to either the Ga vacancy or As interstitial.¹⁴⁾ In our work, the deep level around 0.6 eV near the surface in the annealed implanted GaAs films may indicate the existence of arsenic-rich or precipitate related defects.

Figure 2 shows the temperature-dependent resistance on the films. The samples were As^+ -implanted S.I. GaAs and annealed at 600°C for 30 min. The carrier-transport mechanisms of as-implanted GaAs and annealed sample

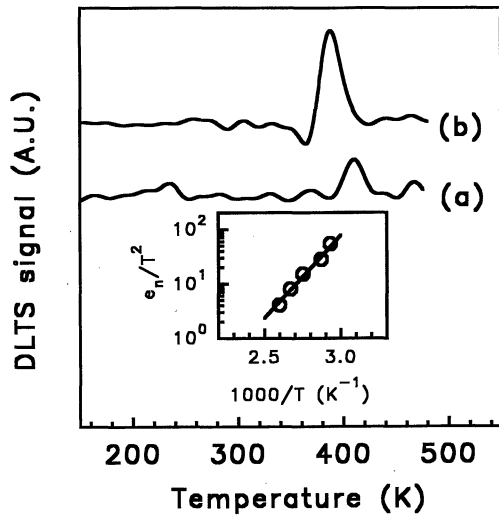


Fig. 1. The DLTS for As⁺-implanted samples. (a): the as-implanted GaAs, (b): the sample annealed at $T_a = 600^\circ\text{C}$ for 30 minutes. The inset shows the Arrhenius plot for sample at $T_a = 600^\circ\text{C}$. The rate window is 69315 s^{-1} .

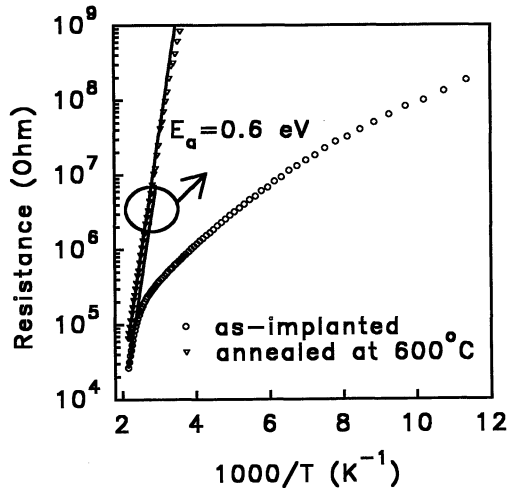


Fig. 2. The temperature-dependent resistance measured on the As⁺-implanted S.I. GaAs. (circle: as-implanted film; triangle-down: sample at $T_a = 600^\circ\text{C}$ for 30 minutes; solid line the curve-fitting of the linear region for the above curves).

are dominated by hopping conduction and active conduction, respectively. The behavior of conduction follows the formula, $R_{\text{Hopping}} = R_0 \exp(B/T^{1/4})$ for hopping conduction and $R_{\text{Active}} = R_{A0} \exp(E_a/kT)$ for active conduction, respectively.^{15, 16} The transport mechanism at temperature above 360 K for the as-implanted GaAs is dominated by active conduction, while at temperature below 360 K the hopping conduction dominates. After annealing at 600°C , only the thermally active conduction can be observed in the film. We can estimate the activation energy, E_a , for both the as-implanted and annealed sample to be about 0.6 eV. The E_a measured by DLTS and temperature-dependent resistance may be the same defect level generated in annealed samples. The disappearance of hopping-conduction phenomenon may indicate that the resistance of the film annealed at 600°C increases.

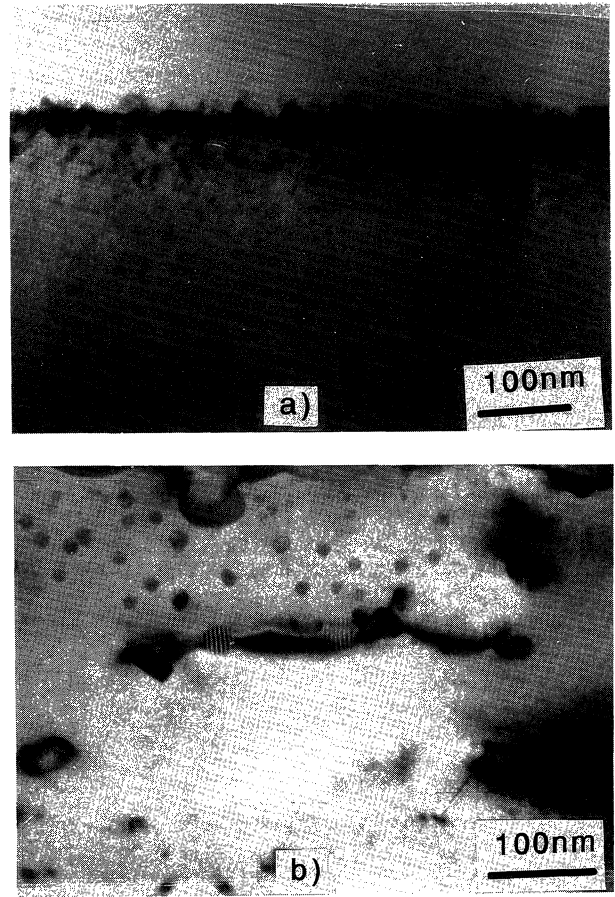


Fig. 3. The cross section micrographs of TEM. (a): as-implanted film; (b): sample at $T_a = 600^\circ\text{C}$ for 30 minutes.

Figure 3(a) shows the TEM image of the amorphous structure of as-implanted GaAs with film thickness of about 140 nm. As the films annealed at 600°C , a lot of As precipitates are accompanied with dislocation defects shown in Fig. 3(b), and the concentration of precipitates is about $7 \times 10^{16}\text{ cm}^{-3}$. And the mean size is about 2–3 nm. The observation of structures and As precipitates in films at $T_a = 600^\circ\text{C}$ has been reported.^{6–10} In addition, to compare with the concentration of As clusters in the LT-MBE GaAs, at $T_a = 600^\circ\text{C}$ it is reported $5 \times 10^{17}\text{ cm}^{-3}$.¹⁹ This value is close to the observed results in As⁺-implanted GaAs film at $T_a = 600^\circ\text{C}$. The As precipitates were previously reported to be 3 m symmetrical rhombohedral As (metallic).¹³ In our experiments from the observations of TEM, DLTS and temperature-dependent resistance measurements we suggest that the near-surface deep level of $E_c - 0.60\text{ eV}$ is responsible for the formations of As precipitates.

In summary, the measurement of temperature-dependent resistance and DLTS on As⁺-implanted GaAs suggest the existence of the deep level defects near the surface with an activation energy around 0.6 eV. After thermal annealing at 600°C , As precipitates with size of 2–3 nm is observed by TEM analysis. The carrier-transport mechanism is dominated by active conduction with the similar activation energy in the as-implanted GaAs measured above 360 K. The hopping-conduction mechanism for the implanted GaAs film diminishes af-

ter annealing at 600°C. Furthermore, the authors are interested in the result that the concentration of As precipitates may depend on the As ion implantation dosage. And the work has been carried out.

We are grateful for the support of National Nanoscale Device Laboratory and for the helpful discussion of professor Ci-Ling Pan about the content. The work is supported by National Science Council of R.O.C. under Grants of NSC85-2215-E009-064.

- 1) Special issue on low temperature grown GaAs and related materials, *J. Electron. Mater.* **22** (1993) 1393.
- 2) M. O. Manasreh, D. C. Look, K. R. Evans and C. E. Stutz: *Phys. Rev. B* **41** (1990) 10272.
- 3) M. Missous and S. O'Hagan: *J. Appl. Phys.* **75** (1994) 3396.
- 4) D. C. Look, D. C. Walter, M. O. Manasreh, J. R. Sizelove, C. E. Stutz and K. R. Evans: *Phys. Rev. B* **42** (1990) 3578.
- 5) A. C. Warren, J. M. Woodall, J. L. Freeouf, D. Grischkowsky, D. T. Mulnturff, M. R. Melloch and N. Otsuka: *Appl. Phys. Lett.* **57** (1990) 1331.
- 6) A. Claverie, F. Namavar and Z. Liliental-Weber: *Appl. Phys. Lett.* **62** (1993) 1271.
- 7) F. Namavar, N. M. Kalkhoran, A. Claverie, Z. Liliental-Weber, E. R. Weber, P. A. Sekula-Moise, S. Vernon and V. Haven: *J. Electron. Mater.* **22** (1993) 1409.
- 8) Z. Liliental-Weber, F. Namavar and A. Claverie: *Ultramicroscopy* **52** (1993) 570.
- 9) A. Claverie, H. Fujioka, L. Laânab, Z. Liliental-Weber and E. R. Weber: *Nuclear Instrum & Methods B* **96** (1995) 327.
- 10) J. Beauvillain, A. Claverie and K. Akmoum: *J. Phys. III France* **2** (1992) 407.
- 11) G. R. Lin, W. C. Chen, C.-S. Chang and C. L. Pan: *Appl. Phys. Lett.* **65** (1994) 3272.
- 12) D. C. Look, Z.-Q. Fang, H. Yamamoto, J. R. Sizelove, M. G. Mier and C. E. Stutz: *J. Appl. Phys.* **76** (1994) 1029.
- 13) D. V. Lang: *J. Appl. Phys.* **45** (1972) 3023.
- 14) A. Mitonneau, G. M. Martin and A. Mircea: *Electron. Lett.* **13** (1977) 191.
- 15) J. J. Mareš, J. Křištofik and V. Šmíd: *Semicond. Sci. Technol.* **7** (1992) 119.
- 16) N. F. Mott and E. A. Davis: *Electronic Processes in Non-Crystalline Materials* (Clarendon, Oxford, 1979) 2nd ed., pp. 7-62.
- 17) K. Xie, Z. C. Huang and C. R. Wie: *J. Electron. Mater.* **20** (1991) 553.
- 18) G. M. Martin, P. Secordel and C. Venger: *J. Appl. Phys.* **53** (1982) 8706.
- 19) J. K. Luo, H. Thomas, D. V. Morgan and D. Westwood: *Appl. Phys. Lett.* **64** (1994) 3614.